2005

Near-Edge X-ray Absorption Fine Structure Study of Ion-beam-induced Phase Transformation in Gd2(Ti1-yZry)2O7

Ponnusamy Nachimuthu
University of Nevada, Las Vegas

S. Thevuthasan
Pacific Northwest National Laboratory

V. Shutthanandan
Pacific Northwest National Laboratory

E. M. Adams
Pacific Northwest National Laboratory

W. J. Weber
Pacific Northwest National Laboratory

Near-edge x-ray absorption fine-structure study of ion-beam-induced phase transformation in Gd2(Ti1−yZry)2O7

P. Nachimuthu, S. Thevuthasan, V. Shutthanandan, E. M. Adams, W. J. Weber et al.

Citation: J. Appl. Phys. **97**, 033518 (2005); doi: 10.1063/1.1840097
View online: http://dx.doi.org/10.1063/1.1840097
View Table of Contents: http://jap.aip.org/resource/1/JAPIAU/v97/i3
Published by the American Institute of Physics.

Near-edge x-ray absorption fine-structure study of ion-beam-induced phase transformation in $Gd_2(Ti_{1-y}Zr_y)_2O_7$

P. Nachimuthu[a)]
Department of Chemistry, University of Nevada, Las Vegas, Nevada 89154 and Lawrence Berkeley National Laboratory, Berkeley, California 94720

S. Thevuthasan, V. Shutthanandan, E. M. Adams, and W. J. Weber
Pacific Northwest National Laboratory, Richland, Washington 99352

B. D. Begg
Australian Nuclear Science and Technology Organization, Menai, New South Wales 2234, Australia

D. K. Shuh
Lawrence Berkeley National Laboratory, Berkeley, California 94720

D. W. Lindle
Department of Chemistry, University of Nevada, Las Vegas, Nevada 89154

E. M. Gullikson and R. C. C. Perera
Lawrence Berkeley National Laboratory, Berkeley, California 94720

(Received 11 August 2004; accepted 2 November 2004; published online 11 January 2005)

The structural and electronic properties of $Gd_2(Ti_{1-y}Zr_y)_2O_7$ ($y=0-1$) pyrochlores following a 2.0-MeV Au^{2+} ion-beam irradiation ($\sim 5.0\times10^{14}$ Au^{2+}/cm^2) have been investigated by Ti $2p$ and O $1s$ near-edge x-ray absorption fine structure (NEXAFS). The irradiation of $Gd_2(Ti_{1-y}Zr_y)_2O_7$ leads to the phase transformation from the ordered pyrochlore structure ($Fd3m$) to the defect fluorite structure ($Fm3m$) regardless of Zr concentration. Irradiated $Gd_2(Ti_{1-y}Zr_y)_2O_7$ with $y\leqslant 0.5$ are amorphous, although significant short-range order is present. Contrasting to this behavior, compositions with $y\geqslant 0.75$ retain crystallinity in the defect fluorite structure following irradiation. The local structures of Zr^{4+} in the irradiated $Gd_2(Ti_{1-y}Zr_y)_2O_7$ with $y\geqslant 0.75$ determined by NEXAFS are the same as in the cubic fluorite-structured yttria-stabilized zirconia ($Y-ZrO_2$), thereby providing conclusive evidence for the phase transformation. The TiO_6 octahedra present in $Gd_2(Ti_{1-y}Zr_y)_2O_7$ are completely modified by ion-beam irradiation to TiO_x polyhedra, and the Ti coordination is increased to eight with longer Ti–O bond distances. The similarity between cation sites and the degree of disorder in $Gd_2Zr_2O_7$ facilitate the rearrangement and relaxation of Gd, Zr, and O ions/defects. This inhibits amorphization during the ion-beam-induced phase transition to the radiation-resistant defect fluorite structure, which is in contrast to the ordered $Gd_2Ti_2O_7$. © *2005 American Institute of Physics*. [DOI: 10.1063/1.1840097]

I. INTRODUCTION

Pyrochlore materials are potentially useful for a range of technological applications that include use as catalysts, fluorescence centers, both cathode and electrolyte materials in solid oxide fuel cells, oxygen-gas sensors for high-radiation environments, and host matrices for the immobilization of actinide wastes.[1–4] Of these, their use in solid oxide fuel cells and as host matrices for actinide wastes are receiving increasing attention because of the recent discoveries showing that the isovalent substitution of Zr for Ti in $Gd_2Ti_2O_7$ results in a four to five orders-of-magnitude increase in the oxygen-ion conductivity at 875 K and in resistance to energetic particle irradiation.[1–4] The mechanisms responsible for the large increase in these properties have been investigated using neutron diffraction, Raman and infrared spectroscopies, extended x-ray absorption fine structure, molecular dynamics, and atomistic simulations.[3–16] These studies show that the increase in the ionic conductivity in pyrochlore is most likely due to the increased oxygen vacancies at the $48f$ site as a result of cation and anion disordering, which are responsible for the increased ionic conductivity.[1–10] The increased radiation tolerance is attributed to the ease of rearrangement and relaxation of Gd, Zr, and O ions/defects within the crystal structure, which inhibits amorphization by causing the irradiation-induced defects to relax and form cation antisite defects and anion Frenkel defects.[2]

Pyrochlores, in general, exhibit $A_2B_2O_6O'$ ($Fd3m$) stoichiometry and are derivatives of the fluorite structure, but with two cations and one-eighth fewer anions. The unit cell contains eight formula units and four nonequivalent sites. Fixing the origin at the B cation, the atoms A, B, O, and O' occupy the $16d$, $16c$, $48f$, and $8b$ sites, respectively. In $Gd_2Ti_2O_7$ and $Gd_2Zr_2O_7$, Gd^{3+} occupies the eight-coordinate $A(16d)$ sites with six $48f$ and two $8b$ oxygen anions forming a distorted cube, whereas $Ti^{4+}(Zr^{4+})$ occupies the six-

a)Electronic mail: PNachimuthu@lbl.gov

coordinate $B(16c)$ sites, which lie adjacent to the vacant $8a$ anion sites, forming distorted octahedra with oxygen anions from the $48f$ sites. Each oxygen anion in the $48f$ and $8b$ sites is tetrahedrally coordinated to two of each Gd^{3+} and Ti^{4+}, and four of Gd^{3+} cations, respectively. The remaining unoccupied $8a$ oxygen site is surrounded by four $Ti^{4+}(Zr^{4+})$ cations. The $48f$ anions are shifted toward the smaller Ti^{4+} cations by the x positional parameter.[16–18] Ion-beam irradiation of $Gd_2(Ti_{1-y}Zr_y)_2O_7$ by 2.0-MeV Au^{2+} ions ($\sim 5.0 \times 10^{14}$ Au^{2+}/cm^2) results in the transformation of the ordered pyrochlore structure ($Fd3m$) into the defect fluorite structure ($Fm3m$) regardless of Zr substitution. Compositions with $y \leqslant 0.5$ become amorphous whereas compositions with $y \geqslant 0.75$ retain their crystalline structure in the defect fluorite structure under identical irradiation conditions ($\sim 5.0 \times 10^{14}$ Au^{2+}/cm^2).[12,13] This structural phase transition from the $Fd3m$ pyrochlore structure to the $Fm3m$ defect fluorite structure involves the randomization of the oxygen ions among the $48f$, $8b$, and $8a$ sites, and the cations between the $16c$ and $16d$ sites.[11–13]

Recently, Chen *et al.*[7,8] reported on the disorder and ion-beam-induced amorphization in $Gd_2(Ti_{1-y}Zr_y)_2O_7$ pyrochlores measured by x-ray photoelectron spectroscopy (XPS). In the O $1s$ XPS spectra for $Gd_2Ti_2O_7$, a broad feature with two components at binding energies (BEs) of ~526 and 531 eV was observed, and these two distinct peaks merged into a single broad peak when 25% Ti was replaced by Zr, suggesting that the environments of oxygen ions have become similar. Recent work on a $Gd_2Ti_2O_7$ single crystal using site-selective near-edge x-ray absorption fine structure (NEXAFS) and XPS showed no anisotropic distribution of Ti and O sites, and additional collaborative studies[19] resolved that the discrepancies in the previous reports[7,8] result from charging effects during XPS and surface contamination. A similar approach to that described above is used to understand disorder and ion-beam-induced phase transformation in the $Gd_2(Ti_{1-y}Zr_y)_2O_7$ pyrochlores and their role in radiation tolerance.

The availability of synchrotron radiation for x-ray absorption spectroscopic measurements has made NEXAFS a powerful tool for developing a detailed understanding of the electronic and structural properties of materials.[19,20] X-ray absorption originates because of the excitation of core electrons from a particular atomic core level to the unoccupied electronic states, which can make this technique atom specific. Therefore, the structural and electronic properties of $Gd_2(Ti_{1-y}Zr_y)_2O_7$ ($y=0-1$) pyrochlores following a 2.0-MeV Au^{2+} ion-beam irradiation ($\sim 5.0 \times 10^{14}$ Au^{2+}/cm^2) have been investigated by Ti $2p$ and O $1s$ NEXAFS.

II. EXPERIMENT

$Gd_2(Ti_{1-y}Zr_y)_2O_7$ ($y=0-1$) pyrochlores were prepared by a sol-gel route using Ti isopropoxide, tetrabutyl zirconate, and Gd nitrate. The solutions were stir dried and calcined at 975 K for 1 h in air. The calcined material was wet ball milled, dried, pressed into pellets, and sintered in air at 1475 K for 12 h. The pellets were powdered and underwent the same processing steps before sintering in air at 1775 K for 30 h. The pellets were coated with BN, encapsulated in glass, and hot isostatically pressed under Ar at 1775 K for 2 h at 200 MPa to produce fully dense materials. The materials were annealed in air at 1625 K for 48 h to recover oxygen stoichiometry. Glancing-incidence x-ray diffraction revealed single-phase polycrystalline materials with the ordered pyrochlore structure.[11–13] The ion-beam irradiations of $Gd_2(Ti_{1-y}Zr_y)_2O_7$ ($y=0-1$) were performed using the accelerator facilities within the Environmental Molecular Sciences Laboratory at Pacific Northwest National Laboratory (PNNL). The irradiations were carried out at room temperature with a 2.0-MeV Au^{2+} ion beam at normal incidence, and the fluence was approximately 5.0×10^{14} Au^{2+}/cm^2. This fluence is an order of magnitude larger than the threshold required for amorphization of the titanates and produces an amorphous state to a depth of 380 nm in $Gd_2Ti_2O_7$.[12]

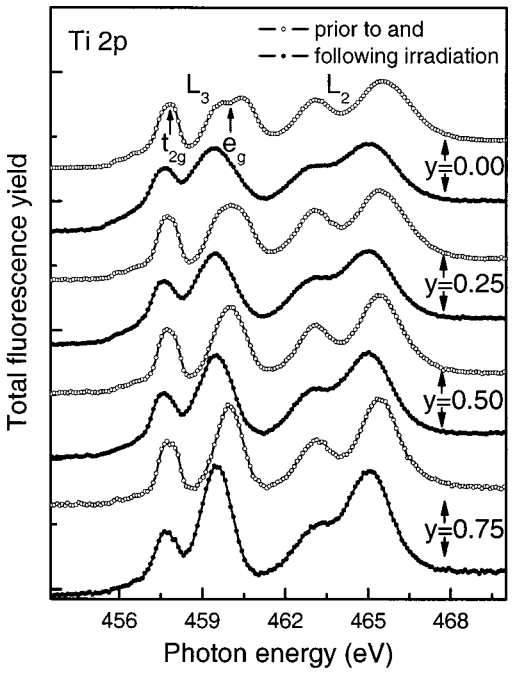

FIG. 1. Titanium $2p$ NEXAFS spectra recorded prior to and following Au^{2+} ion-beam irradiation for $Gd_2(Ti_{1-y}Zr_y)_2O_7$ ($y=0.0$, 0.25, 0.5, and 0.75).

The Ti $2p$ and O $1s$ NEXAFS spectra of $Gd_2(Ti_{1-y}Zr_y)_2O_7$ ($y=0-1$) prior to and following the 2.0-MeV Au^{2+} ion-beam irradiation (5.0×10^{14} Au^{2+}/cm^2) and yttria-stabilized zirconia ($Y-ZrO_2$) were recorded at beamline 6.3.2 of the Advanced Light Source (ALS) at Lawrence Berkeley National Laboratory (LBNL).[21] The total fluorescence yield (TFY) NEXAFS spectra were collected at normal incidence with a photodiode. At these photon energies with TFY detection, the NEXAFS signal originates solely from within the amorphous layer and there is no particular surface sensitivity. Spectra were corrected for the photon flux and normalized to the edge jumps. The photon energy was calibrated to the Ti $2p_{3/2}(t_{2g})$ peak at 457.9 eV and the O K pre-edge transition from $SrTiO_3(100)$ at 530.8 eV. The energy resolution was 125 meV at 530 eV.

III. RESULTS AND DISCUSSION

Figures 1 and 2 show the Ti $2p$ and O $1s$ NEXAFS of

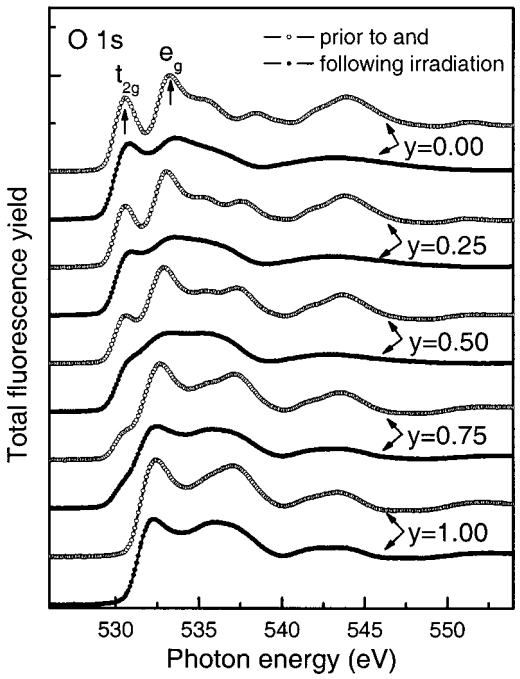

FIG. 2. Oxygen 1*s* NEXAFS spectra recorded prior to and following Au^{2+} ion-beam irradiation for $Gd_2(Ti_{1-y}Zr_y)_2O_7$ (y=0.0, 0.25, 0.5, 75, and 1.0).

$Gd_2(Ti_{1-y}Zr_y)_2O_7$ (y=0–1) prior to and following the 2.0-MeV Au^{2+} ion-beam irradiation (5.0×10^{14} Au^{2+}/cm^2). The assignments of Ti 2*p* and O 1*s* NEXAFS features are made based on a symmetry-determined molecular-orbital model obtained using the linear combination of atomic-orbital method for the octahedral $(TiO_6)^{8-}$-ion cluster in TiO_2.[19,20,22,23] The Ti 2*p* and O 1*s* NEXAFS, in general, probe the unoccupied $2t_{2g}$ (Ti 3*d*+O 2*p*π), $3e_g$ (Ti 3*d* +O 2*p*σ), $3a_{1g}$ (Ti 4*s*+O 2*p*σ), and $4t_{1u}$ (Ti 4*p*+O 2*p*π) states. The ground state of $Gd_2(Ti_{1-y}Zr_y)_2O_7$ consists mainly of $Ti^{4+}:(2p_{3/2,1/2})3d^0-O^{2-}:2p^6$. Spin-orbit interaction splits the Ti 2*p* into $2p_{3/2}(L_3)$ and $2p_{1/2}(L_2)$ states separated by ~5.4 eV. The features labeled as L_3 and L_2 for $Gd_2(Ti_{1-y}Zr_y)_2O_7$ predominantly result from transitions to the final states, $Ti^{4+}:(2p_{3/2,1/2})^{-1}3d^1-O^{2-}:2p^6$, where $(2p_{3/2,1/2})^{-1}$ denotes a hole in the $2p_{3/2}$ or $2p_{1/2}$ state. The t_{2g} and e_g transitions result from transitions to the final states, $Ti^{4+}:(2p_{3/2})^{-1}3d(2t_{2g})^1-O^{2-}:2p^6$ and $Ti^{4+}:(2p_{3/2})^{-1}-3d(3e_g)^1-O^{2-}:2p^6$, respectively. The energy separation between t_{2g} and e_g states is related to the crystal-field strength. The e_g states, which consist of d_{z^2} and $d_{x^2-y^2}$ orbitals, are directed towards ligand anions and are more sensitive to deviations from the octahedral symmetry of Ti. Consequently, the splitting of e_g states into d_{z^2} and $d_{x^2-y^2}$ provides a measure of the degree of distortion from the octahedral site symmetry. The features labeled as t_{2g} and e_g in O 1*s* NEXAFS for $Gd_2(Ti_{1-y}Zr_y)_2O_7$ result from transitions to the final states, $Ti^{4+}:3d(2t_{2g})^1-O^{2-}:(1s)^{-1}-2p^6$ and $Ti^{4+}:3d(3e_g)^1-O^{2-}:(1s)^{-1}2p^6$, respectively, where $(1s)^{-1}$ denotes a hole in the O 1*s* shell (Fig. 2).[19,20,22,23] The separation between t_{2g} and e_g states is 2.7 eV for $Gd_2Ti_2O_7$, which is a direct measure of the crystal-field strength of the TiO_6 octahedra.

Ion-beam irradiation of $Gd_2(Ti_{1-y}Zr_y)_2O_7$ (y=0–1) by 2.0-MeV Au^{2+} results in a significant modification of Ti 2*p* NEXAFS features compared to the spectra obtained prior to irradiation (Fig. 1). The energy separation between t_{2g} and e_g states, which is related to the crystal-field strength, is ~2.3 and ~1.8 eV for $Gd_2(Ti_{1-y}Zr_y)_2O_7$ prior to and following irradiation, respectively. An energy shift of ~0.1 eV towards lower energy for the transitions to the t_{2g} states and line broadening of all the NEXAFS features for irradiated $Gd_2(Ti_{1-y}Zr_y)_2O_7$ are observed. These changes in the features of the NEXAFS spectra occur for all Zr concentrations. The splitting of e_g states into d_{z^2} and $d_{x^2-y^2}$ indicative of the distortion from perfect octahedral site symmetry is less prominent for irradiated $Gd_2(Ti_{1-y}Zr_y)_2O_7$ as Zr substitution increases. This is also manifested in the intensities of the transitions to the e_g states relative to the t_{2g} states, which are progressively enhanced by the increasing overlap of the transitions to d_{z^2} and $d_{x^2-y^2}$ states for the irradiated $Gd_2(Ti_{1-y}Zr_y)_2O_7$ with increasing Zr substitution. These results indicate that the TiO_6 octahedra present in $Gd_2(Ti_{1-y}Zr_y)_2O_7$ are completely modified by ion-beam irradiation to TiO_x polyhedra, and the Ti coordination is increased to eight with longer Ti–O bond distances.

The O 1*s* NEXAFS features for $Gd_2(Ti_{1-y}Zr_y)_2O_7$ (y =0–1) are also significantly modified following the 2.0-MeV Au^{2+} ion-beam irradiation (5.0×10^{14} Au^{2+}/cm^2) (Fig. 2). The spectra for compositions with $y\leqslant0.5$ are completely broadened and have no fine features compared to the spectra prior to irradiation. This contrasts with the spectra with $y\geqslant0.75$, in which all the spectral features are clearly present following the ion-beam irradiation, although the relative intensities of the features are different. This suggests that compositions with $y\leqslant0.5$ are no longer crystalline following irradiation but retain some short-range order, as shown in the Ti 2*p* NEXAFS spectra. However, the compositions with $y\geqslant0.75$ retain their crystallinity, although the changes in spectral intensities in the O 1*s* NEXAFS indicate a phase transformation from the ordered pyrochlore structure ($Fd3m$) to the defect fluorite structure ($Fm3m$) following irradiation. These results are in agreement with previous studies by glancing-incidence x-ray diffraction suggesting that the pyrochlores with $y\geqslant0.75$ were transformed into a radiation-resistant defect fluorite structure ($Fm3m$) following the 2.0-MeV Au^{2+} ion-beam irradiation (5.0×10^{14} Au^{2+}/cm^2) at room temperature.[11–13]

To understand the phase transformation of $Gd_2(Ti_{1-y}Zr_y)_2O_7$ from the ordered pyrochlore structure ($Fd3m$) to the defect fluorite structure ($Fm3m$) induced by the Au^{2+} ion-beam irradiation, the O 1*s* NEXAFS for Y–ZrO_2 in Fig. 3 is compared to the spectra from $Gd_2Ti_2O_7$ and $Gd_2Zr_2O_7$, both prior to and following ion-beam irradiation. The structure of Y–ZrO_2 is cubic fluorite with each Zr^{4+} ion in regular eightfold-coordinated sites with Zr–O distances of equal length.[24,25] $Gd_2Ti_2O_7$ becomes amorphous following ion-beam irradiation, and the subsequent O 1*s* NEXAFS spectrum is completely broadened, thus it is difficult to obtain meaningful specific information from the spectral features. Contrasting with $Gd_2Ti_2O_7$, irradiated $Gd_2Zr_2O_7$ shows a first narrow feature at 532.3 eV, which is close to 532.2 eV observed for Y–ZrO_2. This same feature is also observed at 532.5 eV for $Gd_2Zr_2O_7$ prior to irradiation.

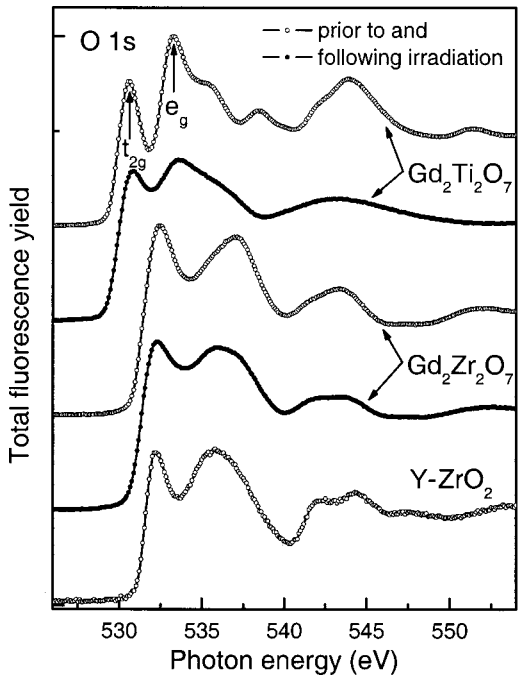

FIG. 3. Comparison of the O 1*s* NEXAFS spectra recorded prior to and following Au^{2+} ion-beam irradiation for $Gd_2Ti_2O_7$ and $Gd_2Zr_2O_7$. The spectrum of yttria-stabilized zirconia ($Y-ZrO_2$) is shown for comparison.

The ion-beam irradiation results in an energy shift of ~0.2 eV towards lower energy. A similar shift is also found for the $y=0.75$ composition. The O 1*s* spectral profiles for the irradiated compositions with $y \geqslant 0.75$ are similar to the spectrum of $Y-ZrO_2$. This confirms that the coordination environment of Zr^{4+} in the irradiated $Gd_2(Ti_{1-y}Zr_y)_2O_7$ with $y \geqslant 0.75$ is the same as in $Y-ZrO_2$ and provides strong evidence for a phase transformation from the ordered pyrochlore structure (*Fd*3*m*) to the defect fluorite structure (*Fm*3*m*) following ion-beam irradiation.

The structural phase transition from the *Fd*3*m* pyrochlore structure to the *Fm*3*m* defect fluorite structure induced by ion-beam irradiation involves the randomization of oxygen ions among the 48*f*, 8*b*, and 8*a* sites, and the cations between the 16*c* and 16*d* sites.[11] Our previous investigations[19,26] of single-crystal $Gd_2Ti_2O_7$ and polycrystalline $Gd_2(Ti_{1-y}Zr_y)_2O_7(y=0-1)$ pyrochlores by Ti 2*p* and O 1*s* NEXAFS and XPS show that Ti^{4+} ions in $Gd_2Ti_2O_7$ occupy octahedral sites with a tetragonal distortion, which is induced by the vacant 8*a* oxygen sites located in the *ab* plane adjacent to the TiO_6 octahedra. With increasing substitution of Zr for Ti in $Gd_2(Ti_{1-y}Zr_y)_2O_7$, the tetragonal distortion in the TiO_6 octahedra decreases and coordination of Zr increases from six to nearly eight. Migration of oxygen ions either from 48*f* or 8*b* sites to vacant 8*a* oxygen sites to compensate for increased coordination of Zr reduces the number of vacant 8*a* oxygen sites, which decreases tetragonal distortion in the TiO_6 octahedra with increasing substitution of Zr for Ti in $Gd_2(Ti_{1-y}Zr_y)_2O_7$. A decrease of tetragonal distortion by the rearrangement of oxygen ions in the TiO_6 octahedra gradually introduces more disorder around Ti with increasing substitution of Zr in $Gd_2(Ti_{1-y}Zr_y)_2O_7$. This in turn suggests that $Gd_2Ti_2O_7$ and $Gd_2Zr_2O_7$ are ordered and relatively less ordered pyrochlore-structured oxides, respectively. Furthermore, Ti^{4+} ions occupy octahedral sites contrasting with both Gd^{3+} and Zr^{4+}, which occupy eightfold and/or nearly eightfold sites. The similarity between cation sites and the degree of disorder in the pyrochlore-structured $Gd_2Zr_2O_7$ facilitate the rearrangement and relaxation of Gd, Zr, and O ions/defects within the crystal structure. This inhibits amorphization during the ion-beam-induced phase transition to the radiation-resistant defect fluorite structure. This contrasts with the ordered pyrochlore-structured $Gd_2Ti_2O_7$, where there is a significant energy barrier between cation sites. This is apparent as a function of Zr substitution for Ti in $Gd_2(Ti_{1-y}Zr_y)_2O_7$ following ion-beam irradiation, in which compositions with $y \leqslant 0.5$ are no longer crystalline; whereas those with $y \geqslant 0.75$ retain their crystallinity. These results and observations are in excellent agreement with recent conclusions suggesting that the susceptibility to ion-beam-induced amorphization and structural disordering of zirconate $A_2Zr_2O_7$ pyrochlores (A=La, Nd, Sm, and Gd) are related to the structural deviation from the ideal fluorite structure as reflected by the positional parameter, x, of the oxygen ions from the 48*f* sites.[5]

IV. CONCLUSIONS

Ti 2*p* and O 1*s* NEXAFS spectra show that phase transformations occur from the ordered pyrochlore structure (*Fd*3*m*) to the defect fluorite structure (*Fm*3*m*) following a 2.0-MeV Au^{2+} ion-beam irradiation (5.0×10^{14} Au^{2+}/cm^2) of $Gd_2(Ti_{1-y}Zr_y)_2O_7$ regardless of the Zr concentration. The irradiated $Gd_2(Ti_{1-y}Zr_y)_2O_7$ with $y \leqslant 0.5$ are amorphous although significant short-range order is retained. Contrasting with this behavior, compositions with $y \geqslant 0.75$ retain crystallinity following ion-beam irradiation. The structures of Zr^{4+} in the irradiated $Gd_2(Ti_{1-y}Zr_y)_2O_7$ with $y \geqslant 0.75$ are nearly the same as in cubic fluorite-structured yttria-stabilized zirconia ($Y-ZrO_2$) providing clear evidence for the phase transformation. The TiO_6 octahedra present in $Gd_2(Ti_{1-y}Zr_y)_2O_7$ is completely modified by the ion-beam irradiation to TiO_x polyhedra, and the Ti coordination is increased to eight with longer Ti–O bond distances. The similarity between cation sites and the degree of disorder in $Gd_2Zr_2O_7$ facilitate the rearrangement and relaxation of Gd, Zr, and O ions/defects. This inhibits amorphization during the ion-beam-induced phase transition to the radiation-resistant defect fluorite structure contrasting with the ordered $Gd_2Ti_2O_7$.

ACKNOWLEDGMENTS

This work was supported by Nevada DOE EPSCoR State-National Lab Partnership Grant No. DE-FG02-01ER45898; the DOE BES Division of Materials Sciences and Engineering and the DOE BER EMSL User Facility at PNNL under Contract No. DE-AC06-76RLO-1830; and the DOE BES Divisions of Materials Sciences and Engineering at the ALS and Chemical Sciences, Geosciences, and Biosciences by Contract No. DE-AC03-76SF00098 at LBNL.

[1]R. C. Ewing, W. J. Weber, and J. Lian, J. Appl. Phys. **95**, 5949 (2004).

[2]W. J. Weber and R. C. Ewing, Science **289**, 2051 (2000).
[3]K. E. Sickafus, L. Minervini, R. W. Grimes, J. A. Valdez, M. Ishimaru, F. Li, K. J. McClellan, and T. Hartmann, Science **289**, 748 (2000).
[4]J. A. Purton and N. L. Allan, J. Mater. Chem. **12**, 2923 (2002).
[5]J. Lian, X. T. Zu, K. V. G. Kutty, J. Chen, L. M. Wang, and R. C. Ewing, Phys. Rev. B **66**, 054108 (2002).
[6]J. Lian, L. M. Wang, S. X. Wang, J. Chen, L. A. Boatner, and R. C. Ewing, Phys. Rev. Lett. **87**, 145901 (2001).
[7]J. Chen, J. Lian, L. M. Wang, R. C. Ewing, R. G. Wang, and W. Pan, Phys. Rev. Lett. **88**, 105901 (2002).
[8]J. Chen, J. Lian, L. M. Wang, R. C. Ewing, and L. A. Boatner, Appl. Phys. Lett. **79**, 1989 (2001).
[9]A. Meldrum, C. W. White, V. Keppens, L. A. Boatner, and R. C. Ewing, Phys. Rev. B **63**, 104109 (2001).
[10]C. Heremans, B. J. Wuensch, J. K. Stalick, and E. Prince, J. Solid State Chem. **117**, 108 (1995).
[11]N. J. Hess, B. D. Begg, S. D. Conradson, D. E. McCready, P. L. Gassman, and W. J. Weber, J. Phys. Chem. B **106**, 4663 (2002).
[12]B. D. Begg, N. J. Hess, W. J. Weber, R. Devanathan, J. P. Icenhower, S. Thevuthasan, and B. P. McGrail, J. Nucl. Mater. **288**, 208 (2001).
[13]B. D. Begg, N. J. Hess, D. E. McCready, S. Thevuthasan, and W. J. Weber, J. Nucl. Mater. **289**, 188 (2001).
[14]R. E. Willford and W. J. Weber, J. Am. Ceram. Soc. **82**, 3266 (1999); J. Nucl. Mater. **299**, 140 (2001).
[15]M. Pirzada, R. W. Grimes, L. Minervini, J. F. Maguire, and K. E. Sickafus, Solid State Ionics **140**, 201 (2001).
[16]L. Minervini, R. W. Grimes, and K. E. Sickafus, J. Am. Ceram. Soc. **83**, 1873 (2000).
[17]M. A. Subramanian, G. Aravamudan, and G. V. Subba Rao, Prog. Solid State Chem. **15**, 55 (1983).
[18]Y. Tabira and R. L. Withers, Philos. Mag. A **79**, 1335 (1999).
[19]P. Nachimuthu *et al.*, Phys. Rev. B **70**, 100101 (2004).
[20]J. G. Chen, Surf. Sci. Rep. **30**, 1 (1997).
[21]J. H. Underwood and E. M. Gullikson, J. Electron Spectrosc. Relat. Phenom. **92**, 265 (1998).
[22]D. W. Fischer, J. Phys. Chem. Solids **32**, 2455 (1971).
[23]F. M. F. de Groot, M. O. Figueiredo, M. J. Basto, M. Abbate, H. Petersen, and J. C. Fuggle, Phys. Chem. Miner. **19**, 140 (1992).
[24]S. Ostanin, A. J. Craven, D. W. McComb, D. Valchos, A. Alavi, A. T. Paxton, and M. W. Finnis, Phys. Rev. B **65**, 224109 (2002).
[25]P. K. Schelling, S. R. Phillpot, and D. Wolf, J. Am. Ceram. Soc. **84**, 1609 (2001).
[26]P. Nachimuthu *et al.* J. Phys. Chem. B(2005) in press.